

A Fault Detection and Location Technique for Inverter-Dominated Islanding Microgrids

Chang, Fangyuan; Sun, Hongbo; Kawano, Shunsuke; Nikovski, Daniel; Kitamura, Shoichi; Su, Wencong

TR2022-073 July 22, 2022

Abstract

Microgrids are attracting increasing interest since they are allowed to work under islanding mode by being disconnected from large-scale commercial distribution networks when large disasters occur. However, disconnected microgrids do not contain appropriate protection systems, which in most cases are installed only at distribution substations. Moreover, the fault currents are significantly limited due to the high penetration of inverter-based distributed generators (IBDGs). Therefore, a protection system or scheme targeted at islanding microgrids is required. In this paper, we develop a transient analysis for islanding ungrounded microgrids, in which multiple IBDGs are deployed under different control strategies, during different types of faults. Furthermore, we propose a fault detection and location method based on two-terminal measurements instead of the singleterminal measurements often utilized in conventional protection schemes such as overcurrent protection. The proposed method does not rely on heavy information exchange. We monitor zero-sequence components, negative-sequence components, and phase currents for locating different types of faults in islanding microgrids. It is verified in our simulation study that the proposed method works well in islanding microgrids with lower fault current levels.

International Electrical and Energy Conference (CIEEC) 2022

© 2022 MERL. This work may not be copied or reproduced in whole or in part for any commercial purpose. Permission to copy in whole or in part without payment of fee is granted for nonprofit educational and research purposes provided that all such whole or partial copies include the following: a notice that such copying is by permission of Mitsubishi Electric Research Laboratories, Inc.; an acknowledgment of the authors and individual contributions to the work; and all applicable portions of the copyright notice. Copying, reproduction, or republishing for any other purpose shall require a license with payment of fee to Mitsubishi Electric Research Laboratories, Inc. All rights reserved.

A Fault Detection and Location Technique for Inverter-Dominated Islanding Microgrids

Fangyuan Chang
Department of Electrical Engineering
University of Michigan-Dearborn
Dearborn, MI 48128, USA
fychang@umich.edu

Hongbo Sun
Data Analytics Group
Mitsubishi Electric Research Labs
Cambridge, MA 02139, USA
hongbosun@merl.com

Shunsuke Kawano
Advanced R&D Technology Center
Mitsubishi Electric Corporation
Amagasaki 661-8661, Japan
kawano.shunsuke@dn.MitsubishiElectric.co.jp

Daniel Nikovski
Data Analytics Group
Mitsubishi Electric Research Labs
Cambridge, MA 02139, USA
nikovski@merl.com

Shoichi Kitamura
Advanced R&D Technology Center
Mitsubishi Electric Corporation
Amagasaki 661-8661, Japan
kitamura.shoichi@dw.mitsubishielectric.co.jp

Wencong Su
Department of Electrical Engineering
University of Michigan-Dearborn
Dearborn, MI 48128, USA
wencong@umich.edu

Abstract—Microgrids are attracting increasing interest since they are allowed to work under islanding mode by being disconnected from large-scale commercial distribution networks when large disasters occur. However, disconnected microgrids do not contain appropriate protection systems, which in most cases are installed only at distribution substations. Moreover, the fault currents are significantly limited due to the high penetration of inverter-based distributed generators (IBDGs). Therefore, a protection system or scheme targeted at islanding microgrids is required. In this paper, we develop a transient analysis for islanding ungrounded microgrids, in which multiple IBDGs are deployed under different control strategies, during different types of faults. Furthermore, we propose a fault detection and location method based on two-terminal measurements instead of the single-terminal measurements often utilized in conventional protection schemes such as overcurrent protection. The proposed method does not rely on heavy information exchange. We monitor zero-sequence components, negative-sequence components, and phase currents for locating different types of faults in islanding microgrids. It is verified in our simulation study that the proposed method works well in islanding microgrids with lower fault current levels.

Keywords—*fault detection, fault location, islanding microgrids, inverter-based distributed generators (IBDGs), system protection*

I. INTRODUCTION

Microgrids have been attracting much more attention recently with the development of a renewable-energy-aware society. Microgrids are localized power grids that can disconnect from the traditional power grid to operate autonomously [1] and are thereby able to strengthen grid reliability and mitigate grid disturbance. Additionally, they are considered promising solutions for operating future power systems integrated with distributed generators (DGs) and renewable energy sources (RESs) [2]. The operation of microgrids is very flexible in that they can operate in both grid-connected and islanding modes. However, the characteristics of a microgrid, such as fault levels and control strategies of inverter-based distributed generators (IBDGs), could vary considerably for different operation modes. Therefore, traditional fault protection schemes may not be applicable to islanding microgrids.

Specifically, fault levels are significantly different in each mode. The fault currents of larger magnitudes (10–50 times the full-load current) are available to activate the traditional overcurrent protection device in grid-connected mode; however, fault currents of only about 5 times the full-load current are available in an islanding microgrid [3]. Especially in an islanding microgrid with high penetration of IBDGs, the maximum output fault current is generally limited to 1.2–2 times that of the rated current. Nevertheless, traditional overcurrent protection devices are usually set to operate at 2–10 times the full-load current [4], which cannot detect and protect islanding microgrids. Moreover, the control techniques of IBDGs are also different in each mode. The common control strategies for IBDGs include PQ control (grid feeding) and VF control (grid following) [5]. PQ control can supply constant power with a reference of active power and reactive power. VF control can regulate the voltage and frequency of IBDG through a voltage control loop and current control loop. All the IBDGs in a microgrid can be operated under PQ control in grid-connected mode, while an IBDG under VF control is required to support the grid voltage in islanding mode. The control strategies of IBDGs could also have a significant impact on fault behaviors [6]. Both of the aforementioned factors lead to new technical challenges to fault detection and location, especially in islanding microgrids. Therefore, an effective fault detection and location method for islanding microgrids needs to be established.

A few existing works scrutinize the fault characteristics of microgrids integrated with IBDGs. In paper [2], a study of the fault characteristics of microgrids dominated by IBDGs with different control strategies is investigated. However, the discussion involves a microgrid model with only two IBDGs and a single transmission line, which cannot represent a typical microgrid model without loss of generality. Papers [7] and [8] examine the fault characteristics of IBDGs with the impacts of fault current limiters (FCLs), whereas a fault detection and location method is still unknown. A fault detection method for an islanding microgrid is developed in paper [9] that leverages the phase differences between the pre-fault bus voltage and the positive-sequence current fault component of the feeders, but the differences among the major types of faults are ignored.

F. Chang conducted the research during her internship at MERL.

To alleviate the limitations in the aforementioned literature, we propose a new fault detection and location technique based on dynamic characteristics of the microgrid electromagnetic transient model at the microsecond level. First, a transient analysis is developed for islanding ungrounded microgrids during faults where multiple IBDGs are deployed under different control strategies. FCLs are adopted to protect IBDGs. With data collected by each sensor deployed at every terminal, we can obtain useful information on transient signal patterns for different fault scenarios, including the major types of grounded and short-circuit faults. Finally, we propose an effective fault detection and location method for islanding microgrids based on the measurements of zero-sequence components, negative-sequence components, and phase currents. Unlike the single-terminal measurements often leveraged in conventional protection, such as overcurrent protection, the proposed method adopts two-terminal measurements but without heavy information exchange. The rest of the paper is organized as follows: section II presents the modeling of islanding microgrids and IBDGs, section III introduces the proposed fault detection and location method for islanding microgrids, and section IV concludes our study in this manuscript.

II. MODELING OF ISLANDING MICROGRIDS

A. Problem Description and Assumptions

Japanese distribution networks are usually grounded at the distribution substations. Protection relays such as overcurrent relays and over-voltage ground relays are installed at the distribution substations and the customer sides. A part of the distribution network starts islanding operation when or after an outage occurs. Therefore, an extra protection scheme is required for the islanding microgrids disconnected from the main grids when a disaster or blackout occurs. We assume that the islanding microgrids are equipped with both traditional synchronous generators (SGs) and inverter-based RESs, which is common in practice. One of the inverters of the RESs is VF-controlled and others are PQ-controlled when the microgrid is operated in islanding mode. All inverters are installed with their own FCL.

B. Control Strategies of IBDGs

VF control and PQ control are two major control strategies for IBDGs. A VF-controlled inverter is also known as a grid forming inverter, which is employed to support the autonomous operation of microgrids in islanding mode. An islanding microgrid needs to greatly meet all the load requirements while keeping voltage and frequency at referred values. VF control is usually utilized for controllable power such as fuel cells and micro-gas turbines [5]. The control block diagram of VF-controlled IBDGs is described in Fig. 1. A PQ-controlled inverter, also known as a grid-following inverter, is usually used for intermittent power generation such as PV generation or wind turbines to follow power references [10]. It can maximize the utilization of renewable energy with intermittency. The control block diagram is described in Fig. 2.

In grid-connected mode, all the IBDGs should be under PQ control since the frequency and voltage of the microgrid should follow the main grid. PQ-controlled inverters inject maximum power into the microgrid to achieve economic operation. The microgrid moves to islanding mode when it is disconnected from the main grid during a blackout. Then one of the IBDGs in the

microgrid should begin to operate under VF control to support voltage and frequency.

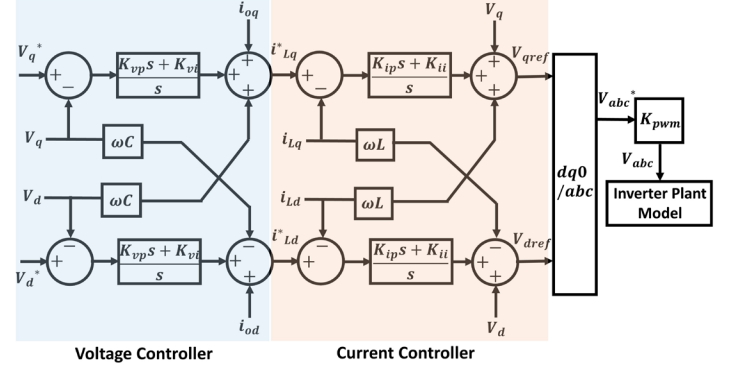


Fig. 1. Control block diagram of VF-controlled IBDGs.

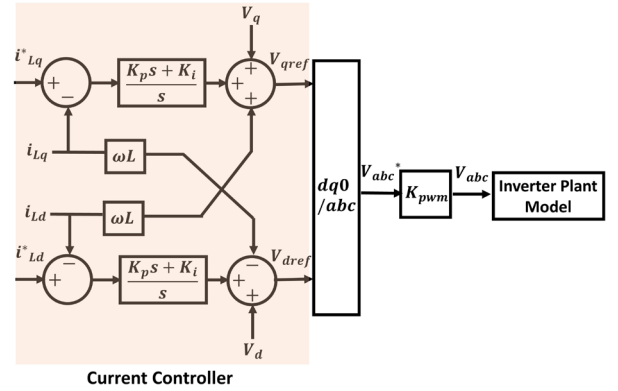


Fig. 2. Control block diagram of PQ-controlled IBDGs.

C. Design of FCLs

A virtual-impedance-based FCL is deployed in each power inverter to suppress the damage of overcurrent. According to (1), a nontrivial virtual-impedance Z_o is activated when the d-axis current I_d and q-axis current I_q of the control current are over their corresponding thresholds I_{thd} and I_{thq} . The configuration of an IBDG without/with FCL is shown in Fig. 3.

$$Z_{FCL} = \begin{cases} 0, & \text{if } I_d < I_{thd} \text{ and } I_q < I_{thq} \\ Z_o, & \text{otherwise} \end{cases} \quad (1)$$

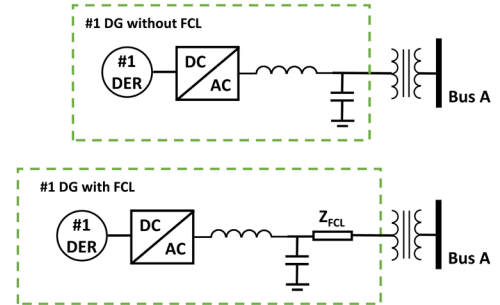


Fig. 3. Configuration of an IBDG without/with FCL.

D. Zero-Sequence and Negative-Sequence Equivalent Circuit

In Japanese microgrids, generators and loads are usually ungrounded. A Delta-Y-connected transformer is often installed at the output of each generator. Considering that zero-sequence current cannot flow through a Delta-Y-connected transformer, the zero-sequence equivalent circuit of DGs is equal to an open circuit. An example is shown in Fig. 4. Suppose a fault voltage

is imposed on branch C_1C . From the zero-sequence fault model in Fig. 4(b), we can expect that the zero-sequence fault currents flowing into different terminals could be from different directions, which provides information for locating the fault.

Negative-sequence current can flow through a Delta-Y-connected transformer, which burdens the modeling of a negative-sequence equivalent circuit. The negative-sequence model of IBDGs is investigated in [7] and [11] and is shown in Fig. 5. Of special note, the control block of VF-controlled IBDGs loses controllability of the negative-sequence circuit, and the negative-sequence impedance is defined by the filter rather than by the control block.

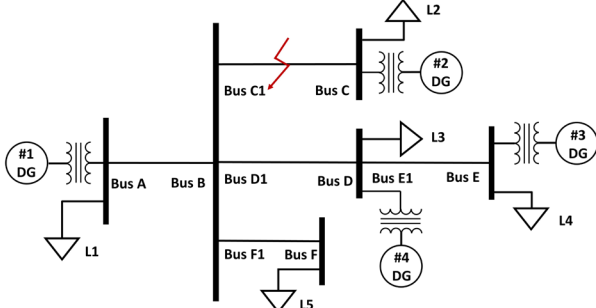


Fig. 4. (a) Original microgrid model.

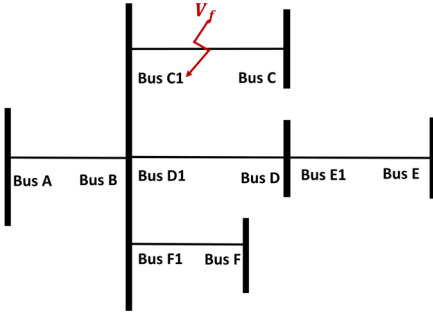


Fig. 4. (b) Zero-sequence fault model.

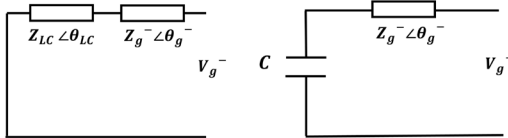


Fig. 5. Negative-sequence equivalent model of VF-controlled IBDGs (left) and PQ-controlled IBDGs (right).

III. A FAULT DETECTION AND LOCATION METHOD

The microgrid electromagnetic transient model is adopted to analyze at the microsecond level the transient process of a microgrid during a fault. With data collected by each sensor deployed at every terminal, we can obtain useful information on transient signals for fault detection and location. The common faults that happen in microgrids can be classified into unsymmetrical faults and symmetrical faults. The unsymmetrical faults include a single line-to-ground short circuit, line-to-line short circuit, and double line-to-ground short circuit; the symmetrical faults usually refer to a three-phase short circuit. We investigate the fault detection and location method for the two major types of faults separately in the following subsections.

A. Unsymmetrical Faults

The islanding microgrid with multiple RESs and SGs in Fig. 6 is simulated using Simscape Electrical Library. Suppose DG #1 is under VF control, DGs #2 and #3 are traditional SGs, and DG #4 is under PQ control. It can be theoretically concluded from the zero-sequence fault model that the directions of the zero-sequence current are opposite *only* at the two ends of the faulted branch, which holds for even a limited fault-current level. In the simulation, suppose the system starts at $t = 0$ s and a single line-to-ground fault happens respectively on different branches at $t = 0.1$ s. The phase diagram of the zero-sequence current in each case is visualized in Fig. 7: (a) fault happens on branch AB; (b) fault happens on branch C_1C ; (c) fault happens on branch D_1D ; (d) fault happens on branch E_1E . In Fig. 7, each arrow represents the zero-sequence current through a different terminal, which is measured at 60ms after the fault happened ($t = 0.16$ s). It can be observed that the directions of the zero-sequence current are opposite *only* at the two ends of the faulted branch. The dynamics of SG and IBDG do not show evident influence on the transient behavior of the faulted branch over the short time horizon at the beginning of the fault.

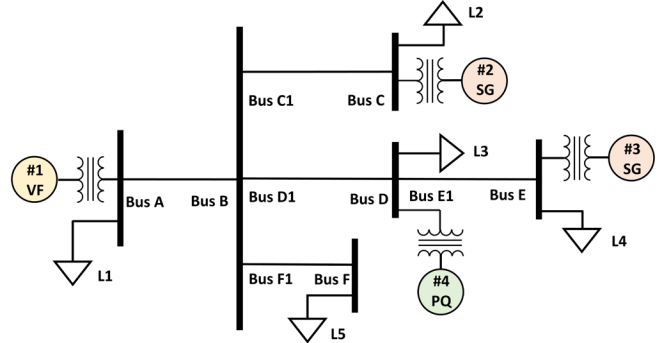


Fig. 6. The simulated microgrid model.

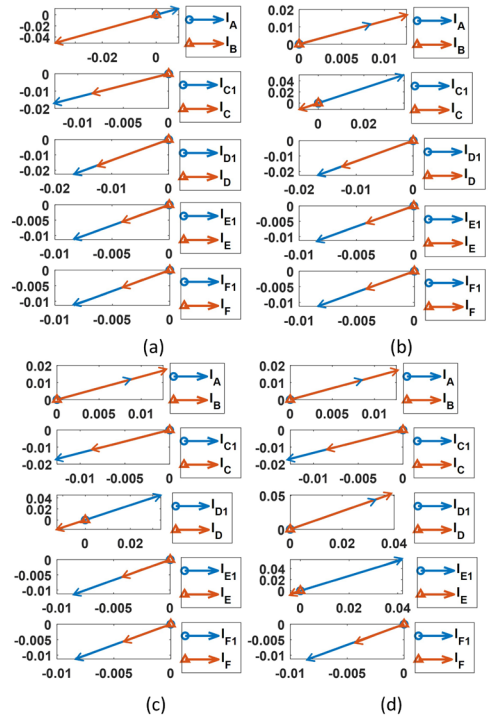


Fig. 7. Phase diagrams of zero-sequence current.

Therefore, a protection scheme can be designed as follows. First, monitor the phase angle difference of the zero-sequence current between the two ends of each branch. It performs chaotically when the microgrid is in normal operation. The reason for this is that the magnitude of the zero-sequence current is infinite small and the angle is unsteady and trivial in a balanced three-phase power system. Conversely, there exist detectable zero-sequence components and the angle becomes steady when a single line-to-ground fault happens. As visualized in Fig. 8, the angle difference is 180 (deg) only on the faulted branch, whereas it is 0 (deg) on other branches, which can locate the fault effectively.

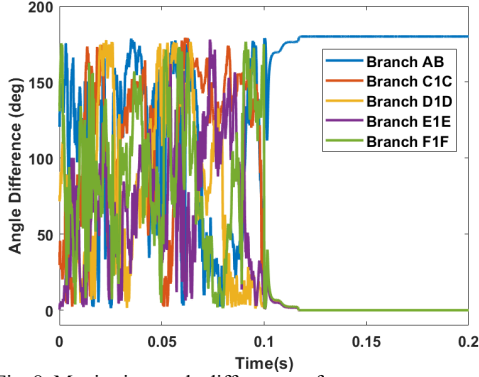


Fig. 8. Monitoring angle differences of zero-sequence current.

B. Symmetrical Faults

The fault location technique based on zero-sequence components cannot be tailored to locate symmetric faults since zero-sequence components are trivial in balanced three-phase power systems. However, during the *transient state immediately after a symmetrical fault* happening (e.g. several microseconds after a fault happening), a negative-sequence fault current (both magnitude and phase angle) shows a significant difference at the two terminals of the faulted branch *only*. It is worthwhile to mention that the above statement does not contradict our basic knowledge that the negative-sequence component is neglectable in a symmetrical circuit system. Here we highlight that our observed period is the transient state right after a fault happening (about 10 ms), when the microgrid system is not strictly symmetrical. Take the model in Fig. 6 as an illustrative example. Suppose a three-phase short-circuit fault happens on different respective branches. The following Tables I–IV present the negative-sequence current through the two terminals of each branch with a fault that happened on different respective branches. The negative-sequence current is measured at 10 ms after the fault happens. The simulation results effectively validate the theoretical conclusion. Moreover, it is observed that the dynamics of SG and IBDG do not show evident influence on the transient behavior of the faulted branch over the short time horizon at the beginning of fault.

TABLE I. CURRENT MEASUREMENT DURING A FAULT HAPPENING ON BRANCH AB

Branch	Current of Terminal 1		Current of Terminal 2	
	Magnitude(A)	Angle(deg)	Magnitude(A)	Angle(deg)
AB	19.66	144.66	426.37	-179.39
C ₁ C	224.14	-179.38	224.14	-179.38
D ₁ D	203.74	-179.39	203.74	-179.39
E ₁ E	210.74	-179.36	210.74	-179.36
F ₁ F	1.51	0.77	1.51	0.78

TABLE II. CURRENT MEASUREMENT DURING A FAULT HAPPENING ON BRANCH C₁C

Branch	Current of Terminal 1		Current of Terminal 2	
	Magnitude(A)	Angle(deg)	Magnitude(A)	Angle(deg)
AB	20.83	145.62	20.83	145.62
C ₁ C	218.89	4.19	259.14	-179.17
D ₁ D	237.34	-178.97	237.34	-178.97
E ₁ E	243.50	-179.18	243.50	-179.18
F ₁ F	1.81	0.86	1.81	0.93

TABLE III. CURRENT MEASUREMENT DURING A FAULT HAPPENING ON BRANCH D₁D

Branch	Current of Terminal 1		Current of Terminal 2	
	Magnitude(A)	Angle(deg)	Magnitude(A)	Angle(deg)
AB	20.83	145.62	20.83	145.62
C ₁ C	259.14	-179.17	259.14	-179.17
D ₁ D	240.61	3.69	237.34	-178.97
E ₁ E	243.50	-179.18	243.50	-179.18
F ₁ F	1.81	0.86	1.81	0.93

TABLE IV. CURRENT MEASUREMENT DURING A FAULT HAPPENING ON BRANCH E₁E

Branch	Current of Terminal 1		Current of Terminal 2	
	Magnitude(A)	Angle(deg)	Magnitude(A)	Angle(deg)
AB	26.59	144.17	26.59	144.17
C ₁ C	225.55	-179.64	225.55	-179.64
D ₁ D	203.24	4.80	203.24	4.80
E ₁ E	196.79	5.13	287.87	-179.07
F ₁ F	1.46	-1.30	1.45	-1.32

A protection scheme is proposed that relies on the measurement of magnitude differences of negative-sequence current between the two ends of each branch. The negative-sequence components are ignorable when the microgrid is under normal operation, whereas they are detectable when a fault happens. As shown in Fig. 9, the magnitude difference of the faulted branch is significantly larger than that of other branches, which locates the fault efficiently.

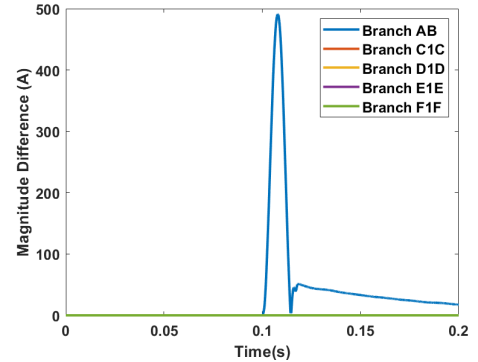


Fig. 9. Magnitude differences of negative-sequence current.

C. A Special Conclusion for Three-Phase Grounded Faults

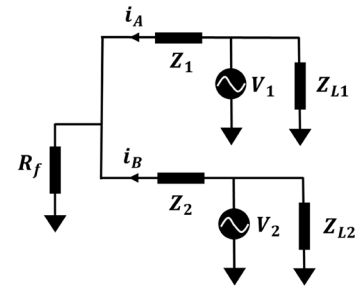


Fig. 10. An equivalent circuit diagram of a microgrid with a three-phase grounded fault.

We discuss another power detection and location technique especially for three-phase grounded faults in this section. Taking one phase as an example, a microgrid with a three-phase grounded fault can be simplified as in the circuit diagram in Fig. 10. R_f is the resistance of the grounded fault. Other notations are introduced in Fig. 10.

The output voltages of all DGs through transformers are usually required to be or be close to a unified value in a microgrid. Here we assume that the voltages of all DGs through transformers are regulated to be the same value, i.e., $V_1 = V_2 = V_m \cos(\omega t + \theta)$. Then the state equation of the circuit model is shown as:

$$\begin{pmatrix} \dot{i}_A \\ \dot{i}_B \end{pmatrix} = \begin{pmatrix} -(R_1 + R_f)/L_1 & -R_f/L_1 \\ -R_f/L_2 & -(R_2 + R_f)/L_2 \end{pmatrix} \begin{pmatrix} i_A \\ i_B \end{pmatrix} + V_m \cos(\omega t + \theta) \quad (2)$$

R_1, L_1, R_2, L_2 are resistance and inductance of the equivalent line impedances. The solutions are shown as follows.

Suppose

$$i_A = i_A^{(1)} + i_A^{(2)}, i_B = i_B^{(1)} + i_B^{(2)} \quad (3)$$

where $i_A^{(1)}$ and $i_B^{(1)}$ are special solutions (ZSR), and $i_A^{(2)}$ and $i_B^{(2)}$ are complementary solutions (ZIR).

$$i_A^{(1)} = (2(\lambda_2 - a)\mu_1 - (\lambda_1 + \lambda_2 + 2a)\mu_2)/(\lambda_2 - \lambda_1) \quad (4)$$

$$i_B^{(1)} = (-2(\lambda_1 - a)\mu_1 + (\lambda_1 + \lambda_2 - 2a)\mu_2)/(\lambda_2 - \lambda_1) \quad (5)$$

$$i_A^{(2)} = e^{-\lambda_2 t}, i_B^{(2)} = -e^{-\lambda_2 t} \quad (6)$$

where

$$a = -(R_1 + R_f)/L_1, b = -R_f/L_1 \quad (7)$$

$$\lambda_{1,2} = (-(R_1 + R_f)/L_1 - (R_2 + R_f)/L_2 \pm \sqrt{\Delta})/2 \quad (8)$$

$$\Delta = \left(\frac{R_1 + R_f}{L_1}\right)^2 + \left(\frac{R_2 + R_f}{L_2}\right)^2 + \frac{2R_f^2 - 2R_1R_2 - 2R_f(R_1 + R_2)}{L_1L_2} \quad (9)$$

$$\mu_1 = V_m/z_1 \cdot \sin(\omega t + \theta + \varphi_1) - e^{-\lambda_1 t} \sin(\theta + \varphi_1) \quad (10)$$

$$\mu_2 = V_m/z_2 \cdot \sin(\omega t + \theta + \varphi_2) - e^{-\lambda_2 t} \sin(\theta + \varphi_2) \quad (11)$$

$$z_1 = (\omega^2 + \lambda_1^2)^{1/2}, z_2 = (\omega^2 + \lambda_2^2)^{1/2} \quad (12)$$

$$\varphi_1 = \tan^{-1}(\lambda_1/\omega), \varphi_2 = \tan^{-1}(\lambda_2/\omega) \quad (13)$$

It is not rigorous to define and leverage the concept of the phase angle of phase currents i_A and i_B due to the existence of harmonics. Instead, we use the sign of i_A and i_B to describe their characteristics. Assume that the reference direction for current i_A and i_B is as marked in Fig. 10. Then the signs of i_A and i_B are always opposite when there is no fault happening. Moreover, it can be known from the above derivations that the signs of i_A and i_B are not always opposite when the following assumptions hold: (a) the attenuation terms are not dominant in i_A and i_B ; (b) $\varphi_1 \approx \pi/4$ or $\varphi_2 \approx 0$ or $\varphi_2 \approx \pi$ or $(\lambda_2 - a)(-1/a - 2a/b) = (a - \lambda_1)(1/a - 2a/b)$. The ratio R/X of a microgrid usually ranges 0.1–10 [12]. As for a small fault resistance, assumption (a) and $\varphi_2 \approx 0$ in assumption (b) hold. Therefore, it is concluded that i_A and i_B are not always opposite when a three-phase grounded fault happens.

This conclusion is validated by simulation tests using Simulink. First, we test multiple scenarios with different line impedances and initial phase angles using the simplified circuit in Fig. 10. The simulation results are shown in Fig. 11. The curves in (a) and (b) plotted by the same color represent i_A and i_B in the same scenario. It is observed that the signs of i_A and i_B are not opposite. In practice, a three-phase grounded fault can be identified by monitoring the real-time phase current. We quantify the signs of the phase current and calculate the

difference in it between the two ends of each branch, which is notated by DS_c .

$$DS_c(t) = \left| \frac{I_M(t)}{|I_M(t)|} - \frac{I_N(t)}{|I_N(t)|} \right| \quad (14)$$

where I_M and I_N are the currents through the two ends of branch MN.

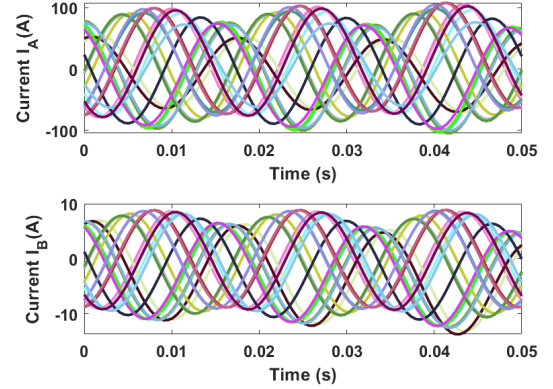


Fig. 11. Comparison between i_A and i_B under multiple scenarios.

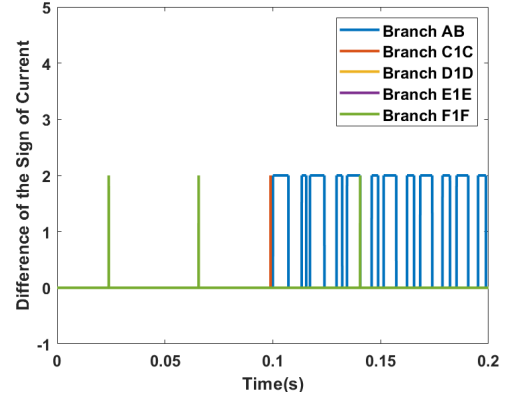


Fig. 12. Monitoring magnitude differences of current.

Take the model in Fig. 6 as an illustrative example. The DS_c of each branch is plotted in Fig. 12. It is observed that DS_c is transitioning between 0 and 2 for the faulted branch and always equals 0 for the other branches (it equals 2 very occasionally due to noise). This phenomenon can validate our derivation. Then it can be concluded that this technique can effectively locate three-phase grounded faults that happen in microgrids.

IV. CONCLUSION

Japanese distribution networks are grounded at the distribution substations, and protection relays are often installed at the distribution substations and the customer sides. A part of the distribution network starts islanding its operation when or after an outage occurs, which requires an extra protection scheme. In this paper, we develop a transient analysis for islanding ungrounded microgrids during different types of faults, where multiple IBDGs are deployed under different control strategies and the effects of FCLs of the IBDGs are considered. A fault detection and location method based on the measurements of zero-sequence components, negative-sequence components, and phase current is proposed for islanding microgrids. The effectiveness of the method is verified in our simulation study. Future work will test the proposed

method on microgrids with larger scales and more complicated topologies.

References

- [1] Office of Electricity, "The Role of Microgrids in Helping to Advance the Nation's Energy System," [Online]. Available: <https://www.energy.gov/oe/activities/technology-development/grid-modernization-and-smart-grid/role-microgrids-helping>
- [2] M. A. Uddin Khan, Q. Hong, A. Dyško, C. Booth, B. Wang and X. Dong, "Evaluation of Fault Characteristic in Microgrids Dominated by Inverter-Based Distributed Generators with Different Control Strategies," 2019 IEEE 8th International Conference on Advanced Power System Automation and Protection (APAP), 2019, pp. 846-849.
- [3] S. Chowdhury, S.P. Chowdhury, P. Crossley, Microgrids and active distribution networks. The Institution of Engineering and Technology, London, United Kingdom, 2009.
- [4] A.A. Memon, and K. Kauhaniemi, "A critical review of AC Microgrid protection issues and available solutions," in Electric Power Systems Research 129, pp. 23-31, 2015.
- [5] B. Ren, X. Tong, S. Tian and X. Sun, "Research on the Control Strategy of Inverters in the Micro-Grid," in Asia-Pacific Power and Energy Engineering Conference, 2010, pp.1-4.
- [6] M. A. Haj-ahmed and M. S. Illindala, "The influence of inverter-based DGs and their controllers on distribution network protection," 2013 IEEE Industry Applications Society Annual Meeting, 2013, pp. 1-9.
- [7] Z. Shuai, C. Shen, X. Yin, X. Liu and Z. J. Shen, "Fault Analysis of Inverter-Interfaced Distributed Generators With Different Control Schemes," in IEEE Transactions on Power Delivery, vol. 33, no. 3, pp. 1223-1235, June 2018.
- [8] W. Guo, L. Mu and X. Zhang, "Fault Models of Inverter-Interfaced Distributed Generators Within a Low-Voltage Microgrid," in IEEE Transactions on Power Delivery, vol. 32, no. 1, pp. 453-461, Feb. 2017.
- [9] Z. Liang, L. Mu, F. Zhang, H. Zhou, X. Zhang, "The fault detection method of islanded microgrid with the V/f controlled distributed generation," in International Journal of Electrical Power & Energy Systems, 112, pp.28-35, 2019.
- [10] Z. Afshar, M. M. Zadeh, S. M. T. Bathaee and G. B. Gharehpetian, "Primary and Secondary Frequency Control of Low-Inertia Microgrids with Battery Energy Storage and Intermittent Renewable Energy Resources," 2020 11th Power Electronics, Drive Systems, and Technologies Conference (PEDSTC), 2020, pp. 1-6.
- [11] P. Kundur, N. J. Balu, and M. G. Lauby, Power System Stability and Control. New York, NY, USA: McGraw-Hill, 1994.
- [12] M.A. Hossain, H.R. Pota, W. Issa, M.J. Hossain, "Overview of AC microgrid controls with inverter-interfaced generations," in Energies, 10(9), pp.1300, 2017.